Author(s): Sihvola, Ari

Title: Homogenization principles and effect of mixing on dielectric behavior

Year: 2013

Version: Pre-print

Please cite the original version:

Sihvola, Ari. 2013. Homogenization principles and effect of mixing on dielectric behavior. Photonics and Nanostructures - Fundamentals and Applications. Volume 11, Issue 4. P. 364-373. ISSN 1569-4410 (printed). DOI: 10.1016/j.photonics.2013.01.004.

Homogenization principles and effect of mixing on dielectric behavior

Ari Sihvola

Aalto University School of Electrical Engineering
Department of Radio Science and Engineering
Box 13000, FI–00076 AALTO, Finland

Abstract

This paper consists of two parts. First, a review of classical mixing principles lists the multitude of the various ways to characterize the effective permittivity of heterogeneous materials. Different connections between the various mixing formulas are underlined and the homogenization principles are classified into families of mixing rules. The second part emphasizes and analyzes the richness of the manner how the mixing process is able to create new types of dielectric behaviors, in particular with respect to enhancement of dielectric polarization, shifts of the dispersion parameters, and emergence of new effects in electrical response.

Keywords: mixing formulas, homogenization, polarizability, Maxwell Garnett, Bruggeman, dispersion models, percolation, emergence

1. Introduction

It is conceptually and practically easy to compute the density of a given sample of heterogenous medium: it is the volume average of the densities of the components that constitute the medium. However, not all intensive physical properties are as straighforward to homogenize as mass density. The calculation of the effective "electrical density", in other words the permittivity of heterogeneities, is an example of such a case.

Needless to say, knowledge of the effective electrical properties of materials are needed in a myriad of fields and applications. The understanding of wave interaction with natural materials is essential in remote sensing of the environment requiring the effective description of geophysical media like snow, ice, precipitation, vegetation, etc. In biological and living matter the multiscale messiness of structural heterogeneities cause significant challenges for understanding the electromagnetic field behavior. And of course in metamaterials research, the effective characterization of a composite formed by complex, resonating, and interacting elements may succeed only after substantial simplifying assumptions.

Homogenization theories for dielectric properties have a long history. Pioneering works on this topic appeared already in the 19th century authored by people like Mossotti, Clausius, L.V. Lorenz, H.A. Lorentz, and Lord Rayleigh. Brosseau [1] has depicted the history of homogenization principles as a play with five scenes. The first one is the J.C. Maxwell Garnett formula to predict the macroscopic permittivity of a two-phase mixture. The next step came along with D.A.G. Bruggeman who developed an "effective medium approximation" for the homogenization problem. After the analysis and theories of bounding principles by Beran, Hashin, Shtrikman, and Bergman, the fourth stage was the understanding of the phenomenon of percolation. Finally, the advent of computational electromagnetics with powerful computers and efficient numerical codes opened unforeseen views for the dielectric homogenization research effort.

To this picture one could add another phase in the path towards better understanding of heterogeneities, which we are presently experiencing. The recent progress in homogenization principles has been particularly boosted in connection of materials with complicated responses. Starting in the late 1980's, much electromagnetics research focused on chiral and bianisotropic materials. In that connection, the homogenization principles needed to be generalized to account for anisotropic and magnetoelectric couplings. The developments in the present century in materials research have expanded this line of studies to such an extent that it is not unfair to talk about a new electromagnetics paradigm: metamaterials research.

The history of effective material properties in the context of electromagnetics has been told from several perspectives. The homogenization problem is indeed a classical problem in statistical physics [2]. References [1, 3, 4, 5, 6, 7] provide more detailed information about the history and past achievements about electromagnetic homogenization.

The inherent limitation of the macroscopic, coarse-grained description of the medium is that the inhomogeneity scale is much smaller than the wavelength of the operating field. The mixing rules are often based on static field solutions for the structure. Hence, once the operating frequency increases sufficiently, the validity of the result is lost. It is not easy to give an exact upper frequency limit for effective permittivity of the sample because the exact response of a randomly heterogeneous medium is beyond analysis. However, the following estimate is often used: the size of an inclusion in the mixture must not exceed a tenth of the wavelength in the effective medium. However, this very crude estimate is popular among people working with positive-permittivity, isotropic, and low-loss materials for which the effective permittivity does not display very surprising effects. Consequently, in the homogenization business of metamaterials, one may need to require much stricter limitations in terms of allowed ratio between the inclusion size and the wavelength, even down to one over a hundred [8, 9].

This presentation reviews most important dielectric homogenization principles and their generalizations. There is no single solution for the effective characterization of materials with random structure and the question arises about the capability of a given mixing formula to explain the macroscopic properties of a given sample. However, it is astonishing that often very simple-looking mix-

ing rules work well. It is also extremely interesting that these mixing principles may predict very unexpected behavior types for the composite which very often correspond to real physical phenomena. These will be introduced and analyzed in the present paper.

2. Classical mixing formulas

Mixing rules enumerate the effective permittivity ε_{eff} (or any other macroscopic material parameter) of a mixture, or of a heterogeneous medium that consists of medium components that are dielectrically different from each other. Let us start with two-phase mixtures, one of which forms the background (environment), and the other one is embedded as a guest, forming the inclusions phase. Let the dielectric relative permittivity of the host material be ε_e, and that of the guest ε_i. The volume fraction of the inclusions is denoted by p. Then the fractional volume occupied by the host is $1-p$. The treated mixtures are three-dimensional unless otherwise stated.

In the following, the permittivities are *relative*, in other words dimensionless quantities. This is to avoid keeping the free-space permittivity ε_0 along in the results. Furthermore, the time-harmonic convention $\exp(\mathrm{j}\omega t)$ is followed which leads to negative imaginary part of the permittivity for dissipative media. This makes the definition $\varepsilon_{\text{eff}} = \varepsilon'_{\text{eff}} - \mathrm{j}\varepsilon''_{\text{eff}}$ convenient.

Maxwell Garnett formula

The prediction for the effective permittivity ε_{eff} according to the Maxwell Garnett formula is [10]

$$\varepsilon_{\text{eff}} = \varepsilon_e + 3p\varepsilon_e \frac{\varepsilon_i - \varepsilon_e}{\varepsilon_i + 2\varepsilon_e - p(\varepsilon_i - \varepsilon_e)} \tag{1}$$

for this mixture under consideration.

If the roles of the host and guest are reversed in the Maxwell Garnett formula, we arrive at the so-called inverse Maxwell Garnett rule, which consequently reads

$$\varepsilon_{\text{eff}} = \varepsilon_i + 3(1-p)\varepsilon_i \frac{\varepsilon_e - \varepsilon_i}{\varepsilon_e + 2\varepsilon_i - (1-p)(\varepsilon_e - \varepsilon_i)} \tag{2}$$

Predictions for a two-phase mixture effective permittivity may differ quite strongly depending on whether the Maxwell Garnett or its inverse is applied, especially if the permittivity contrast is strong between the two phases. This is natural due to the very different morphology of the two structures: the environment forms a continuous phase whereas the inclusions are separated islands. In terms of connectivity, the two scenarios are labeled 0–3 and 3–0 composites.

Bruggeman formula

According to the Bruggeman (symmetric) mixing rule [11], the effective permittivity follows the relation

$$(1-p)\frac{\varepsilon_e - \varepsilon_{\text{eff}}}{\varepsilon_e + 2\varepsilon_{\text{eff}}} + p\frac{\varepsilon_i - \varepsilon_{\text{eff}}}{\varepsilon_i + 2\varepsilon_{\text{eff}}} = 0 \tag{3}$$

The essence of the Bruggeman formalism is the equality between the two phases in the mixture. There is neither host nor guest. An interpretation of (3) is that the homogenized medium itself is the background against which polarizations are measured. Then it also follows that no "inverse Bruggeman formula" exists: the mixture and its complement (which emerges through the transformation $\varepsilon_i \to \varepsilon_e,\ \varepsilon_e \to \varepsilon_i,\ p \to 1-p$) lead the the same equation. Hence the connectivity character of the Bruggeman model is fundamentally different from Maxwell Garnett. Both components form a three-dimensional continuum and the connectivity is rather of 3–3 type as opposed to the raisin-pudding (0–3) or the Swiss cheese (3–0) composites.

Coherent potential formula

One further formula which is relevant in the theoretical studies of wave propagation in random media is the so-called Coherent potential formula [12]. It can be written in the form

$$\varepsilon_{\text{eff}} = \varepsilon_e + f(\varepsilon_i - \varepsilon_e)\frac{3\varepsilon_{\text{eff}}}{3\varepsilon_{\text{eff}} + (1-f)(\varepsilon_i - \varepsilon_e)} \tag{4}$$

A family of mixing rules has been presented in [13] which contains all the previous aspects of dielectric mixing rule. For the case of isotropic spherical inclusions ε_i in the isotropic environment ε_e, the formula looks like

$$\frac{\varepsilon_{\text{eff}} - \varepsilon_e}{\varepsilon_{\text{eff}} + 2\varepsilon_e + \nu(\varepsilon_{\text{eff}} - \varepsilon_e)} = p\frac{\varepsilon_i - \varepsilon_e}{\varepsilon_i + 2\varepsilon_e + \nu(\varepsilon_{\text{eff}} - \varepsilon_e)} \tag{5}$$

and includes a dimensionless parameter ν. For different choices of ν, the various mixing rules are recovered: $\nu = 0$ gives the Maxwell Garnett rule, $\nu = 2$ gives the Bruggeman formula, and $\nu = 3$ gives the Coherent potential approximation.

Multiphase mixtures

The previous mixing rules can be rather straightforwardly generalized into multiphase mixtures. For example, in a mixture where only the environment is of 3-dimensionally continuous connectivity and N other phases are as spherical inclusions, the Maxwell Garnett formula attains the form

$$\frac{\varepsilon_{\text{eff}} - \varepsilon_e}{\varepsilon_{\text{eff}} + 2\varepsilon_e} = \sum_{n=1}^{N} p_n \frac{\varepsilon_{i,n} - \varepsilon_e}{\varepsilon_{i,n} + 2\varepsilon_e} \tag{6}$$

where p_n is the volume fraction of the inclusions of the nth phase in the mixture, and $\varepsilon_{i,n}$ is its permittivity.

Shape effects of inclusions

The spherical shape for the inclusions is symmetric, simple, and natural. By numerical efforts, this assumption can be relaxed, but it turns out that simple analytical solutions can be found also for the electrostatic problem with

ellipsoidal geometries. An ellipsoid allows two more degrees of freedom over sphere, and contains practical special cases, like discs and needles.

The important parameters in the geometry of an ellipsoid are its depolarization factors. If the semi-axes of an ellipsoid in the three orthogonal directions are a_x, a_y, and a_z, the depolarization factor N_x (the factor in the x-direction) is [3]

$$N_x = \frac{a_x a_y a_z}{2} \int_0^\infty \frac{ds}{(s+a_x^2)\sqrt{(s+a_x^2)(s+a_y^2)(s+a_z^2)}} \tag{7}$$

For the other depolarization factor N_y (N_z), interchange a_y and a_x (a_z and a_x) in the above integral. The three depolarization factors for any ellipsoid satisfy

$$N_x + N_y + N_z = 1 \tag{8}$$

A sphere has three equal depolarization factors of $1/3$. The other two special cases are a disc (depolarization factors $1, 0, 0$), and a needle with circular cross section $(0, 1/2, 1/2)$. For ellipsoids of revolution, prolate and oblate ellipsoids, closed-form expressions for the integral (7) can be found in [14].

The normalized polarizability of a homogeneous dielectric sphere with permittivity ε in free space reads $\alpha = 3(\varepsilon - 1)/(\varepsilon + 2)$. For the ellipsoid the polarizability depends on the direction of the field excitation:

$$\alpha_j = \frac{\varepsilon - 1}{1 + N_j(\varepsilon - 1)}, \quad i = x, y, z \tag{9}$$

Furthermore, the mixture with aligned ellipsoids of permittivity ε_i are embedded in the environment ε_e is anisotropic with different permittivity components along the principal directions. The Maxwell Garnett formula for this mixture is

$$\varepsilon_{\mathrm{eff},x} = \varepsilon_e + p\varepsilon_e \frac{\varepsilon_i - \varepsilon_e}{\varepsilon_e + (1-p)N_x(\varepsilon_i - \varepsilon_e)} \tag{10}$$

with the respective relations for $\varepsilon_{\mathrm{eff},y}$ and $\varepsilon_{\mathrm{eff},z}$. For a random mixture, the effective permittivity is isotropic as the three polarization components have to be averaged [3]. For further analysis about the effects of ellipsoidal shapes, see [15, 16].

The result (10) is particularly instructive because it not only describes the aligned ellipsoid mixture but it also opens up the Maxwell Garnett model into other spatial dimensions. For example, a cylinder with circular cross section is a two-dimensional sphere for electric field perpendicular to the cylinder axis. Since the depolarization factor for this case is $N_x = N_y = 1/2$ (and the axis-directed factor is $N_z = 0$), we have the two-dimensional Maxwell Garnett mixing rule from (10)

$$\varepsilon_{\mathrm{eff}} = \varepsilon_{\mathrm{e}} + 2p\varepsilon_{\mathrm{e}} \frac{\varepsilon_{\mathrm{i}} - \varepsilon_{\mathrm{e}}}{\varepsilon_{\mathrm{i}} + \varepsilon_{\mathrm{e}} - p(\varepsilon_{\mathrm{i}} - \varepsilon_{\mathrm{e}})} \tag{11}$$

and the one-dimensional case ($N_z = 1$) reads accordingly

$$\varepsilon_{\mathrm{eff}} = \varepsilon_{\mathrm{e}} + p\varepsilon_{\mathrm{e}} \frac{\varepsilon_{\mathrm{i}} - \varepsilon_{\mathrm{e}}}{p\varepsilon_{\mathrm{e}} + (1-p)\varepsilon_{\mathrm{i}}} = \frac{\varepsilon_{\mathrm{i}}\varepsilon_{\mathrm{e}}}{p\varepsilon_{\mathrm{e}} + (1-p)\varepsilon_{\mathrm{i}}} \tag{12}$$

which can be recognized as the effective permittivity of a planar layered structure for polarization perpendicular to the plane.

The world of two-dimensional mixtures is extremely fascinating and would deserve a chapter of its own, especially due to the fact that there exist many fundamental principles—like, for example, the Keller theorem [17]—that do not have any equivalents in three dimension.

Further mixing models

A widely used class of mixing models in remote sensing applications is the "power-law" approximations:

$$\varepsilon_{\text{eff}}^a = p\varepsilon_i^a + (1-p)\varepsilon_e^a \tag{13}$$

As examples, in the Birchak formula [18] the parameter is $a = 1/2$, which means that the volume-weighted square roots of the component permittivities add up to the square root of the effective permittivity. Another known formula is the Looyenga formula [19] for which $a = 1/3$.

Sometimes the simple avarage is used:

$$\varepsilon_{\text{eff}} = p\varepsilon_i + (1-p)\varepsilon_e \tag{14}$$

which corresponds to $a = 1$ in (13). This mixing rule is the exact static solution for a planar mixture with no depolarization (in other words, for the same mixture as in (12) but the field is polarized parallel to the planes). Since the depolarization factor is $N_x = 0$, formula (14) can be recovered from (10).

In geophysical sensing, also other one-third power formulas have been used [20]:

$$\frac{\varepsilon_i - \varepsilon_{\text{eff}}}{\varepsilon_i - \varepsilon_e} = (1-p)\left(\frac{\varepsilon_{\text{eff}}}{\varepsilon_e}\right)^{1/3} \tag{15}$$

and its dual model:

$$\frac{\varepsilon_{\text{eff}} - \varepsilon_e}{\varepsilon_i - \varepsilon_e} = p\left(\frac{\varepsilon_{\text{eff}}}{\varepsilon_i}\right)^{1/3} \tag{16}$$

For more discussion on various mixing models, see [3, Chapter 9].

3. Physical phenomena explained by mixing formulas

The previous chapter showed that there are indeed a large number of mixing models for use in different application domains. Obviously, these formulas are very simple in appearance due to the fact that only dipolar interaction effects were accounted for. Higher-order multipolar and spatial dispersion effects were left out that play an important role for inclusion-rich mixtures. Nevertheless, it is true that many of these rules are surprisingly accurate in predicting the true effective permittivity for a given application.

In this chapter, the focus is on how the mixing process can radically create new type of responses that are displayed by the composite but not present in the constituent materials. This type of emergent behavior is typically affiliated with metamaterials [21].

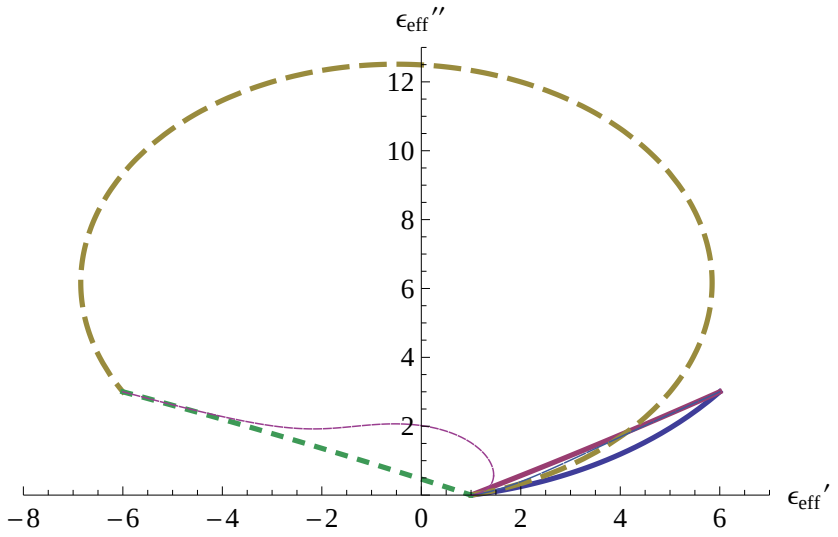

Figure 1: The Hashin–Shtrikman bounds in the complex plane for a mixture of air and lossy medium $\varepsilon = 6 - \mathrm{j} \cdot 3$ (the area between solid lines), and for the mixture of air and lossy plasmonic medium $\varepsilon = -6 - \mathrm{j} \cdot 3$ (dashed lines.) The Bruggeman prediction falls within the bounds in both cases (thin lines). Note the parametric display style of the curves. The curves in the complex $\varepsilon_{\mathrm{eff}}$ plane start from air ($\varepsilon_{\mathrm{e}} = +1 + \mathrm{j} \cdot 0$) and end in the lossy medium ($\varepsilon_{\mathrm{i}} = \pm 6 - \mathrm{j} \cdot 3$).

3.1. Bounds and polarization enhancement

Homogenization literature contains theoretical studies on limits for the effective permittivity of a given random sample. For example, the Hashin–Shtrikman bounds [22] apply for statistically homogeneous and isotropic mixtures. Indeed, the bounds are exactly the Maxwell Garnett (1) and inverse Maxwell Garnett (2) formulas!

For positive permittivity, low-loss materials, these limits may be quite strict. However, for lossy media, or even negative-permittivity media, a very wide range of allowed effective permittivities falls between these limits. This is illustrated in Figure 1, where the dramatic difference of the "ordinary" lossy mixture ($\varepsilon_{\mathrm{i}} = +6 - \mathrm{j} \cdot 3$ with $\varepsilon_{\mathrm{e}} = 1$) and a lossy but plasmonic mixture ($\varepsilon_{\mathrm{i}} = -6 - \mathrm{j} \cdot 3$ with $\varepsilon_{\mathrm{e}} = 1$) can be observed. For the first case, the Hashin–Shtrikman limits are very close to one another, whereas the effective permittivity of the plasmonic mixture has much more freedom. For example, the allowed region is rather "high" in the vertical direction, which means that a plasmonic composite can be made much more lossy than either of its components. The figure also contains the Bruggeman prediction (3) which in both cases lies in its entirety within the allowed region.

In addition to negative-permittivity mixtures, another striking example about loosening of the effective permittivity bounds is the case of mixtures with high dielectric losses. In that case, the counterintuitive behavior that happens in

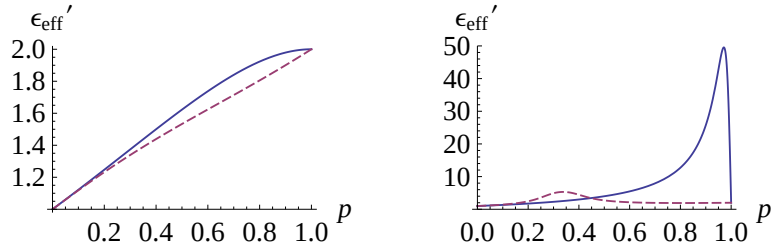

Figure 2: The predictions of the Maxwell Garnett (solid blue) and Bruggeman (dashed red) predictions for fair-loss ($\varepsilon_i = 2 - \mathrm{j}\cdot 2$, left-hand side panel) and high-loss ($\varepsilon_i = 2 - \mathrm{j}\cdot 100$, right-hand side panel) mixtures. For high-loss mixtures, the model predictions differ strongly. Both predict polarization enhancement but at different mixing ratios and of different magnitudes. In both cases, the host medium is assumed to be free space ($\varepsilon_e = 1$).

terms of the magnitude of polarization in the effective medium has been pointed out [23]. Even if it sounds very reasonable that the permittivity of the mixture of two materials with different permittivities would have a value somewhere between these two permittivities, this is not the case for lossy mixtures.

Figure 2 shows the macroscopic permittivity (the real part $\varepsilon'_{\mathrm{eff}}$) of a simple mixture where lossy spherical inclusions (with real part of the permittivity $\varepsilon'_i = 2$) are embedded in lossless background ($\varepsilon_e = 1$). Maxwell Garnett and Bruggeman mixing formulas are applied.

If the losses are sufficiently small (left panel of the figure), both predictions are reasonably similar functions of the volume fraction of the lossy phase. The real part of the effective permittivity increases smoothly from the value 1 to 2. On the other hand, when the losses become large (right panel), the real part may attain values much higher than those of either of the components. This phenomenon is observed for both mixing rules, however, according to the Maxwell Garnett model this enhancement is greatly stronger than in case of the Bruggeman prediction. Also, the maxima take place for different volume fractions.

In [24], a quantitative treatment of this phenomemon can be found. The enhancement effect requires large enough losses. The threshold for Maxwell Garnett is the following for a mixture where the inclusion phase ε_i is lossy ($\varepsilon'_i > 1$) and the environment ε_e lossless, here assumed unity ($\varepsilon_e = 1$): when the imaginary part ε''_i increases beyond the value

$$\varepsilon''_{\mathrm{lim}} = \sqrt{(\varepsilon'_i - 1)(\varepsilon'_i + 2)} \tag{17}$$

a maximum appears (in other words $\varepsilon'_{\mathrm{eff}} > \varepsilon'_i$). This happens at the volume fraction

$$f_{\max} = \frac{|\varepsilon_i - 1||\varepsilon_i + 2|^2 - 3\varepsilon''_i|\varepsilon_i + 2|}{|\varepsilon_i - 1|\left(|\varepsilon_i|^2 + \varepsilon'_i - 2\right)} \tag{18}$$

where the modulus of a complex number $a = a' - \mathrm{j}a''$ is $|a| = \sqrt{a'^2 + a''^2}$.

For this volume fraction of the inclusion phase with permittivity ε_i, the real part of the effective permittivity is

$$\varepsilon'_{\mathrm{eff,max}} = \frac{|\varepsilon_i - 1||\varepsilon_i + 2| - \varepsilon''_i}{2\varepsilon''_i} \tag{19}$$

If the imaginary part of the inclusion phase is increased, the real part $\varepsilon'_{\mathrm{eff}}$ grows to a value approaching $\varepsilon''_i/2$.

3.2. Change of dispersion characteristics in the homogenized mixture

Through the mixing rules, the dielectric dispersion of the homogenized mixture is a nonlinear function of the dispersive properties of the constituent materials. Dispersion may change character in the mixing process. An apt metaphor is that the macroscopic permittivity is like a child that inherits the properties of its parents (from the two component materials composing the mixture). It is true that the properties of the child are functions of those of the earlier generation. But children also rebel against parents and new effects emerge [25].

One example of this phenomenon is a mixture where noble metal inclusions are embedded into a dispersionless dielectric matrix. This composite obeys a different dispersion law than either of the constituents [3]. Metal is a Drude medium with a given plasma frequency. But the composite becomes a Lorentz-dispersive mixture which is characterized by a resonance frequency. It is insulator at low frequencies due to the non-connectivity of the metal inclusions is this raisin-pudding type mixture.

Another striking example of engineered dispersion is the mixing with Debye-type materials. Debye materials (like water) have a relaxation-type dispersion

$$\varepsilon_{\mathrm{Debye}} = \varepsilon_\infty + \frac{\varepsilon_\mathrm{s} - \varepsilon_\infty}{1 + \mathrm{j}\omega\tau} \tag{20}$$

with the static ε_s and high-frequency ε_∞ permittivities and the relaxation time τ.

The mixing process affects the relaxation characteristics as can be seen from the example in Figure 3. There the imaginary part of the permittivity ε'' is displayed as function of frequency ω for bulk medium and mixtures. A water-like Debye medium has high losses at the relaxation frequency ω_{rel}. Also shown are air–Debye mixtures for the case when 10% of the volume is occupied by the liquid phase. The Debye parameters are taken to be those of water at room temperature. The frequency is normalized to the relaxation frequency of bulk liquid, which is around 17 GHz at room temperature for water.

The loss character depends on the model. For the raisin-pudding mixture (water droplet is air), the losses are smallest and they are shifted to high frequencies, and for the complementary case of air bubbles (water as host, air as guest, Swiss cheese) the imaginary part of the permittivity is higher but at the same frequency as the bulk water. The Bruggeman rule gives results between the two Maxwell Garnett models.

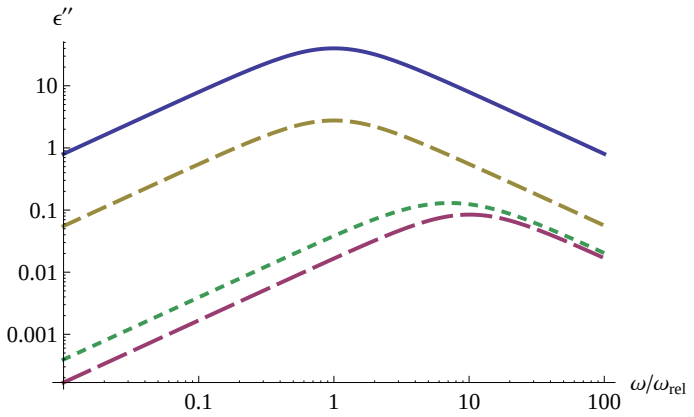

Figure 3: The imaginary part of the permittivity of water-like Debye material over a wide frequency range (solid blue line), and also for the mixture where such material occupies 10 % of the volume in air ($\varepsilon_e = 1$). The mixture is modeled by three approaches: raisin-pudding Maxwell Garnett (droplets in air; long-dashed red line); Swiss-cheese Maxwell Garnett (air bubbles in water; short-dashed yellow); and symmetric Bruggeman (dotted green line).

A third example of a phenomenon how mixing changes the dispersive law is the so-called Maxwell–Wagner effect [26]. This happens in particular in connection with thin layers and membranes that separate lossy domains, for example cells that contain saline liquids, and is often also called interfacial polarization effect.

However, this phenomenon does not require membranes or insulating layers. Again, a simple application of Maxwell Garnett formula reveals the dramatic change of dispersion: Assuming spherical inclusions with complex permittivity $\varepsilon_i' - \mathrm{j}\sigma/(\omega\varepsilon_0)$ embedded in insulating matrix ε_e with volume fraction p, the effective permittivity can be shown to follow a Debye-type dispersion with parameters

$$\varepsilon_\mathrm{s} = \varepsilon_e + \varepsilon_e \frac{3p}{1-p} \tag{21}$$

$$\varepsilon_\infty = \varepsilon_e + 3p \frac{\varepsilon_i' - \varepsilon_e}{\varepsilon_i' + 2\varepsilon_e - p(\varepsilon_i' - \varepsilon_e)} \tag{22}$$

$$\tau = \frac{\varepsilon_i' + 2\varepsilon_e - p(\varepsilon_i' - \varepsilon_e)}{(1-p)\sigma/\varepsilon_0} \tag{23}$$

Note that unlike in the first example of Drude-type inclusions where the result was a Lorentzian composite, now the metallic conductivity of the inclusions leads to a relaxation-type dispersion.

3.3. Red and blueshifts

The geometry and shape of the inclusions in the mixture have also a strong effect on the spectral behavior of the composite. Indeed, the changes can be

seen also in the response of a single inclusion. The polarizability of an ellipsoid (9) is dependent on the depolarization factor but also very nonlinearly on the frequency dependence of the permittivity. Hence changing the shape of the inclusion, plasmonic resonances shift.

Figures 4 and 5 display the effect of the geometry of the nanoparticle on the plasmonic resonance. There the polarizability of a silver nanosphere is shown as function of wavelength. The Drude model fitted [27] to experimental data is used

$$\varepsilon_{\text{Silver}}(\lambda) = \varepsilon_\infty - \frac{(\lambda/\lambda_p)^2}{1 - \mathrm{j}\lambda/\lambda_d} \tag{24}$$

where $\varepsilon_\infty = 5.5$, $\lambda_p = 130\,\text{nm}$, and $\lambda_d = 30\,\mu\text{m}$. This is a fairly good model for the permittivity of silver in the range $320\,\text{nm} < \lambda < 700\,\text{nm}$.

Three shapes are studied: a sphere, a prolate spheroid (needle-like) with axis ratio 2:1, and an oblate spheroid (disk-like) with axis ratio 1:2. The polarizabilities are shown for field excitation along the axis of revolution. It is clearly seen that the plasmonic resonance is red-shifted is the particle is elongated in the field direction, and blue-shifted in the contrary case.

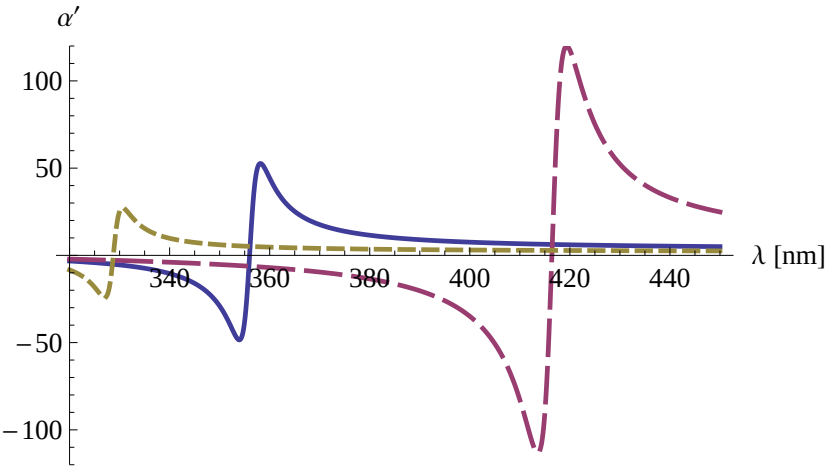

Figure 4: The real part of the polarizability of silver spheres and ellipsoids in air as function of wavelength. Solid blue: sphere; long-dashed red: prolate ellipsoid with axis ratio 2:1 (depolarization factor in the axis direction $N = 0.1736$); short-dashed green: oblate ellipsoid with axis ratio 1:2 (depolarization factor $N = 0.5272$).

3.4. Percolation

In the narrative by Brosseau [1], the fourth stage in the homogenization developments was centered on the phenomenon of percolation. Percolation is a multidisciplinary concept [28, 29]. It is not surprising that percolation appears in different mixing rules in different ways. Coarsely speaking, percolation means that at a certain small change of the structure of the composite, a very abrupt change occurs in the macroscopic behavior. The effective medium may behave

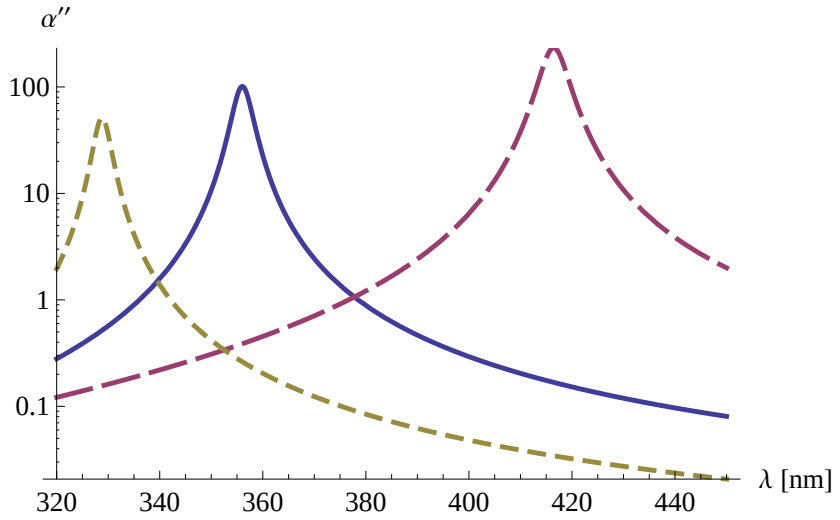

Figure 5: As in Figure 4, for the imaginary part of the polarizability.

totally differently depending on which side of the percolation threshold its state is.

An instructive way of appreciating the connection of mixing rules with percolation is to analyze the general mixing rule (5) that contains the parameter ν. The percolation phenomenon requires very highly contrasting dielectric permittivities in the mixture. Let the dielectric contrast ϵ_i/ϵ_e in become large in (5). Then equation is approximately

$$\frac{\varepsilon_{\text{eff}} - \varepsilon_e}{\varepsilon_{\text{eff}} + 2\varepsilon_e + \nu(\varepsilon_{\text{eff}} - \varepsilon_e)} = p \tag{25}$$

From this ε_{eff} reads

$$\varepsilon_{\text{eff}} = \varepsilon_e \frac{1 + (2-\nu)p}{1 - (1+\nu)p} \tag{26}$$

However, this result breaks down when the denominator reaches the value zero. It is interesting to connect this value for the volume fraction as the percolation threshold point p_c

$$p = p_c = \frac{1}{1+\nu} \tag{27}$$

The threshold depends on ν, in other words on the type of the mixing rule. The threshold varies between $p_c = 1$ (Maxwell Garnett) and $p_c = 0$ ($\nu = \infty$). For example, for the Bruggeman formula ($\nu = 2$), this gives the percolation threshold 0.333 which has been known in the composite materials research for decades. Percolating mixtures, especially in terms of their conductivity, have been analyzed in more detail by McLachlan [30].

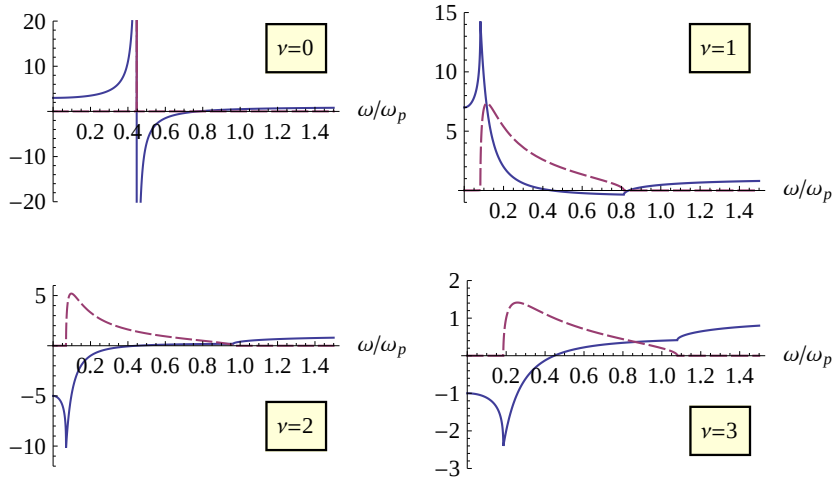

Figure 6: Effective permittivity ($\varepsilon'_{\text{eff}}$: solid line; $\varepsilon''_{\text{eff}}$: dashed line) of Drude spheres in air with volume fraction $p = 0.4$. All other models predict a frequency band with nonzero losses except the Maxwell Garnett formula $\nu = 0$.

3.5. Emergent loss

The various mixing formulas in the family (5) have the common character that for low inclusion loading, they give fairly similar effective permittivity predictions. The linear term in the Taylor expansion (around $p = 0$) is the same independently of ν. However, when p increases, the predictions start to differ for high-contrast mixtures. This discrepancy becomes extreme when plasmonic mixtures are analyzed.

For the case that the inclusion and the background permittivities have different signs, the Maxwell Garnett prediction is that for a particular volume fraction, the effective permittivity grows without limit (in the lossless case). On the other hand, the Bruggeman formula predicts, instead of a singularity, a region where the effective permittivity is complex [31, 32]. In other words, despite real-values elements, the homogenized continuum becomes complex. This type of non-dissipative damping sounds very counter-intuitive.

Let us take a parametric look at how the emergence of the imaginary part into the effective permittivity depends on the type of the mixing formula. For simplicity, let us treat a mixture where lossless Drude-type spheres ($\varepsilon_{\text{i}} = 1 - (\omega_p/\omega)^2$) occupy a volume fraction $p = 0.4$ in air ($\varepsilon_{\text{e}} = 1$). Varying the ν parameter in (5) we capture different mixing rules (Maxwell Garnett for $\nu = 0$, Bruggeman for $\nu = 2$, and Coherent Potential for $\nu = 3$.) The results are displayed in Figure 6.

An interesting phenomenon can be gathered from the figure. All models except Maxwell Garnett predict that there is a frequency band where ε_{eff} becomes complex. This band broadens with increasing ν. In this sense the singularity

in the Maxwell Garnett prediction can be seen as a zero-limit loss band when $\nu \to 0$.

Figure 6 raises also the following question: if mixing rules that are so closely related as these four predict qualitatively different results, how can one trust mixing formulas when they are applied in new territories? Part of the answer is that since the morphologies of all mixtures with a given fractional volume partition are different from each other, they may in particular material combinations behave very differently. Maxwell Garnett has been proven to be surprisingly suited for ordered simple-cubic mixtures, even in the plasmonic case [31]. This is the case in particular for low plasmonic inclusion loadings, for higher concentrations, Maxwell Garnett formula has been generalized to account for higher order corrections.

On the other hand, the range of applicability of the Bruggeman rule falls more into the case of random mixing of spheres that may touch each other and even form clusters. This has been shown in the positive permittivity settings [33]. Touching spheres involve geometric constellations with singular points, and it is known that such special geometries lead to situations where a real-valued negative-permittivity inclusion attains a complex polarizability [34, 35, 36].

The emergence of losses from purely real component materials has to be approached in the realistic setting: in practice, losses are inevitable in the component materials. Then the paradox translates into an enhancement possibility: with extremely small losses to begin with, considerable macroscopic losses can be generated [37]. The relative increase of the loss factor can therefore, by a clever mixing process, be designed to be arbitrarily large.

4. Conclusion

To paraphrase David Bergman [2], the question of permittivity of a composite is a classical problem in physics. The history of dielectric homogenization studies is long and rich, and there is no shortage of mixing principles and dielectric effective medium models to be applied in the various fields of science, technology, biology, or medicine, where the complexity of the medium geometry and structure has to be compressed into a fewer number of coarse-grained quantities. It has been one of the messages of the present paper that despite the formal simplicity of the mixing formulas, their validity and predictive power is fairly strong in several relevant application situations. Furthermore, the applicability of these formulas carries over to other branches of physics, like for modeling of heterogeneous magnetic materials.

Particular attention was paid in the present paper to the qualitatively strong effects that the mixing process may bring forth in the frequency dispersion in the composite. The conducting, relaxation-type, or plasmonic character of the electric response of constituent materials may transform into significantly different type of effective spectral behavior. Conspicuous examples of such an effect were the shift of the relaxation frequency of Debye-type materials from the bulk into the particular state, the appearance of the resonance character of mixtures

with Drude-type isolated inclusions, and the mixing of lossy particles into dielectric matrix which resulted in Maxwell–Wagner type of dispersion typical in biological matter.

It is the obligation of the electromagnetics research community to develop ambitious and mathematically solid first-principles homogenization theories that lead to rigorous effective medium principles. The message of the present paper is that, on the other hand, very often deep insight about the essential macroscopic behavior of real-world materials may be accrued from mixing principles that are based on rather intuitive approaches to the electrophysics of the homogenization problem.

References

[1] C. Brosseau, Modelling and simulation of dielectric heterostructures: a physical survey from an historical perspective, Journal of Physics D: Applied Physics 39 (2006) 1277–1294.

[2] D. J. Bergman, The dielectric constant of a composite material – a problem in classical physics, Physics Reports 43 (9) (1978) 377 – 407.

[3] A. Sihvola, Electromagnetic Mixing Formulas and Applications, Vol. 47 of Electromagnetic Waves Series, IEE Publishing, London, 1999.

[4] R. Landauer, Electrical conductivity in inhomogeneous media, AIP Conference Proceedings 40 (1) (1978) 2–45.

[5] J. Van Kranendonk, J. E. Sipe, Foundations of the macroscopic electromagnetic theory of dielectric media, Progress in Optics XV (1977) 245–350.

[6] A. Lakhtakia (Ed.), Selected papers on linear optical composite materials, Vol. MS120, SPIE Optical Engineering Press, 1996.

[7] G. W. Milton, The Theory of Composites, Cambridge University Press, 2002.

[8] F. Lederer, C. Menzel, C. Rockstuhl, T. Pertsch, Can optical metamaterials be described by effective material parameters?, in: Metamaterials 2009 – 3rd International Congress on Advanced Electromagnetic Materials in Microwaves and Optics, 2009, pp. 11–13, London, UK.

[9] A. Andryieuski, C. Menzel, C. Rockstuhl, R. Malureanu, F. Lederer, A. Lavrinenko, Homogenization of resonant chiral metamaterials, Physical Review B 82 (2010) 235107.

[10] J. C. Maxwell Garnett, Colours in metal glasses and metal films, Transactions of the Royal Society (London) 203 (1904) 385–420.

[11] D. A. G. Bruggeman, Berechnung verschiedener physikalischer Konstanten von heterogenen Substanzen. I. Dielektrizitätskonstanten und Leitfähigkeiten der Mischkörper aus isotropen Substanzen, Annalen der Physik 24 (7-8) (1935) 636–679.

[12] R. J. Elliott, J. A. Krumhansl, P. L. Leath, The theory and properties of randomly disordered crystals and related physical systems, Reviews of Modern Physics 46 (1974) 465–543.

[13] A. Sihvola, Self-consistency aspects of dielectric mixing theories, IEEE Transactions on Geoscience and Remote Sensing 27 (4) (1989) 403–415.

[14] L. D. Landau, E. M. Lifshitz, Electrodynamics of Continuous Media, Second Edition, Pergamon Press, Oxford, 1984.

[15] R. W. Cohen, G. D. Cody, M. D. Coutts, B. Abeles, Optical properties of granular Silver and Gold films, Physical Review B 8 (1973) 3689–3701.

[16] J. G. Yardley, R. C. McPhedran, N. A. Nicorovici, L. C. Botten, Addition formulas and the Rayleigh identity for arrays of elliptical cylinders, Physical Review E 60 (1999) 6068–6080.

[17] J. B. Keller, Conductivity of a medium containing a dense array of perfectly spheres or cylinders or nonconducting cylinders, Journal of Applied Physics 34 (1962) 991–993.

[18] J. R. Birchak, L. G. Gardner, J. W. Hipp, J. M. Victor, High dielectric constant microwave probes for sensing soil moisture, Proceedings of the IEEE 62 (1) (1974) 93–98.

[19] H. Looyenga, Dielectric constants of mixtures, Physica 31 (1965) 401–406.

[20] P. N. Sen, C. Scala, M. H. Cohen, A self-similar model for sedimentary rocks with application to the dielectric constant of fused glass beads, Geophysics 46 (5) (1981) 781–795.

[21] A. Sihvola, Metamaterials in electromagnetics, Metamaterials 1 (1) (2007) 2–11.

[22] Z. Hashin, S. Shtrikman, A variational approach to the theory of the effective magnetic permeability of multiphase materials, Journal of Applied Physics 33 (10) (1962) 3125–3131.

[23] A. Sihvola, How strict are theoretical bounds for dielectric properties of mixtures?, IEEE Transactions on Geoscience and Remote Sensing 40 (4) (2002) 880–886.

[24] K. Kupfer (Ed.), Electromagnetic aquametry, Springer, Heidelberg, 2005, Ch. A. Sihvola: Model systems for materials with high dielectric losses in aquametry, pp. 93–112.

[25] A. Sihvola, Metamaterials: a personal view, Radioengineering 18 (2) (2009) 92–94.

[26] K. W. Wagner, Erklärung der dielektrischen Nachwirkungsvorgänge auf Grund Maxwellscher Vorstellungen, Archiv für Elektrotechnik.

[27] H. Wallén, H. Kettunen, A. Sihvola, Composite near-field superlens design using mixing formulas and simulations, Metamaterials 3 (34) (2009) 129–139.

[28] G. Grimmett, Percolation, Springer, New York, 1989.

[29] D. Stauffer, A. Aharony, Introduction to percolation theory, Taylor & Francis, London and Philadelphia, 1994.

[30] D. S. McLachlan, Equations for the conductivity of macroscopic mixtures, Journal of Physics C: Solid State Physics 19 (1986) 1339–1354.

[31] H. Wallén, H. Kettunen, A. Sihvola, Mixing formulas and plasmonic composites, in: S. Zouhdi, A. Sihvola, A. Vinogradov (Eds.), Metamaterials and plasmonics: fundamentals, modelling, applications, NATO Science for Peace and Security Series, B – Physics and Biophysics, Springer, Dordrecht, 2009, pp. 91–102.

[32] A. Sihvola, Six-dimensional view of dielectric mixtures as metamaterials, European Physical Journal: Applied Physics 46 (32602), 6 pages.

[33] K. Kärkkainen, A. Sihvola, K. Nikoskinen, Analysis of a three-dimensional dielectric mixture with finite difference method, IEEE Transactions on Geoscience and Remote Sensing 39 (5) (2001) 1013 –1018. doi:10.1109/36.921419.

[34] M. Pitkonen, A closed-form solution for the polarizability of a dielectric double half-cylinder, Journal of Electromagnetic Waves and Applications 24 (8-9) (2010) 1267–1277.

[35] N. M. Estakhri, A. Alù, Large absorption efficiency in ultralow loss, composite plasmonic nanoparticles, in: 2012 IEEE International Symposium on Antennas and Propagation, Chicago, IL, USA, July 8-14, 2012.

[36] R. McPhedran, Branch cuts and resonances for metamaterials and plasmonics, in: Proceedings of Croucher Advanced Study Institute Conference, HKUST, Hong Kong, October 3-7, p. 43, 2012.

[37] A. Sihvola, H. Wallén, H. Kettunen, Losses from lossless building blocks?, in: Proceedings of *Metamaterials 2012*, 6th International Congress on Advanced Electromagnetic Materials in Microwaves and Optics, 2012, pp. 261–263.